ELSEVIER

Biochimica et Biophysica Acta 1509 (2000) 167–175

BIOCHIMICA ET BIOPHYSICA ACTA

BBA

www.elsevier.com/locate/bba

A fluorescence study of the interaction and location of (+)-totarol, a diterpenoid bioactive molecule, in model membranes

C. Reyes Mateo [a], Manuel Prieto [b], Vicente Micol [a], Stuart Shapiro [c], José Villalaín [a,*]

[a] *Centro de Biología Molecular y Celular, Campus de Elche, Universidad Miguel Hernández, E-03202 Elche-Alicante, Spain*

[b] *Centro de Química-Física Molecular, Instituto Superior Técnico, Av. Rovisco Pais, P-1049-001 Lisbon, Portugal*

[c] *Institut für orale Mikrobiologie und allgemeine Immunologie, Zentrum für Zahn-, Mund- und Kieferheilkunde der Universität Zürich, Plattenstrasse 11, Postfach, CH-8028 Zürich 7, Switzerland*

Received 13 April 2000; received in revised form 30 June 2000; accepted 17 July 2000

Abstract

(+)-Totarol, a diterpene extracted from *Podocarpus totara*, has been reported as a potent antioxidant and antibacterial agent. Although the molecular mechanism of action of this hydrophobic molecule remains unknown, recent work made in our laboratory strongly suggests that it could be lipid-mediated. Since (+)-totarol contains a phenolic ring, we have studied the intrinsic fluorescent properties of this molecule, i.e., quantum yield, lifetime, steady-state anisotropy and emission spectra, both in aqueous and in phospholipid phases, in order to obtain information on the interaction and location of (+)-totarol in biomembrane model systems. The phospholipid/water partition coefficient of (+)-totarol was found to be very high ($K_p = 1.8 \times 10^4$), suggesting that it incorporates very efficiently into membranes. In order to estimate the transverse location (degree of penetration) of the molecule in the fluid phase of DMPC model membranes, the spin labelled fatty acids 5-NS and 16-NS were used in differential quenching experiments. The results obtained show that (+)-totarol is located in the inner region of the membrane, far away from the phospholipid/water interface. Since (+)-totarol protects against oxidative stress, its interaction with an unsaturated fatty acid, *trans*-parinaric acid, was studied using fluorescence resonance energy transfer. No significant interactions were observed, molecules of *trans*-parinaric acid distributing themselves randomly amongst those of (+)-totarol in the phospholipid membrane.

Keywords: Totarol; Fluorescence spectroscopy; Model membrane; Phospholipid vesicle; *trans*-Parinaric acid

1. Introduction

The diterpenoid (+)-totarol (14-isopropyl-8,11,13-podocarpatrien-13-ol; Fig. 1), extracted from the timber of *Podocarpus totara*, a conifer native of New Zealand, has been reported to be a potent natural antibiotic, active against diverse bacterial species, with minimal inhibitory concentrations as low as 1 μM [1–3]. (+)-Totarol is reportedly active against β-lactam-resistant strains of bacteria and

Abbreviations: DMPC, 1,2-dimyristoyl-*sn*-glycero-3-phosphocholine; DMPG, 1,2-dimyristoyl-*sn*-glycero-3-[phospho-rac-glycerol]; FRET, fluorescence resonance energy transfer; LUV, Large unilamellar vesicles; MLV, Multilamellar vesicles; n-NS, n-(*N*-oxy-4,4-dimethyloxazolidin-2-yl)-stearic acid; PA-DPH, 3-(*p*-6-phenyl-1,3,5-hexatrienyl)-phenylpropionic acid; *t*-PnA, *trans*-parinaric acid

* Corresponding author. Fax: +34-966-658-758; E-mail: boullon@umh.es

0005-2736/00/$ – see front matter
PII: S0005-2736(00)00291-1

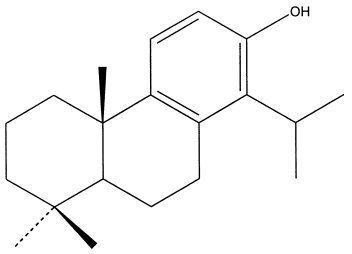

Fig. 1. Chemical structure of (+)-totarol (14-isopropyl-8,11,13-podocarpatrien-13-ol).

this diterpenoid, alone or in combination with other molecules, could be proven useful in countering the problem of increasing bacterial resistance to antibiotics, since its cytotoxicity towards human cell cultures is relatively mild [3,4]. The relationship between the chemistry of (+)-totarol and its antibacterial activity has been the subject of recent investigations [3,5], in the course of which it has been shown that the phenolic moiety is essential for its potent antibacterial effects (cf. [1]). In addition to its antibacterial activity, (+)-totarol has shown itself to be effective for protecting biological systems against oxidative stress [6,7]. The mechanisms of the antibacterial and antioxidant activities of (+)-totarol are not yet understood, though results obtained by Haraguchi et al. [6,7] and in our laboratories [8] suggest that the site of action of (+)-totarol could be the cell membrane.

The primary aim of this work is to quantify the extent and better understand the nature of the interactions and location of (+)-totarol in biomembrane model systems. Since (+)-totarol contains a phenolic ring, its photophysical properties (absorption and fluorescence spectra, fluorescence quantum yield, fluorescence lifetime and steady-state anisotropy) could be used for this purpose. Briefly, the photophysical properties of this molecule have been characterised in homogeneous solvents and in phospholipid model membrane systems. We have also obtained topographical information on (+)-totarol in the phospholipid membrane, i.e., its transverse location, from the intrinsic fluorescence quenching of (+)-totarol by spin-labelled fatty acids. Results show that (+)-totarol is incorporated very efficiently into the membrane and its phenol moiety being located into the inner core distant to the phospholipid/water interface. In addition, since (+)-totarol shows antioxidant properties, its interaction with a model polyunsaturated system (*trans*-parinaric acid) was also studied using fluorescence resonance energy transfer (FRET).

2. Materials and methods

2.1. Materials

(+)-Totarol (14-isopropyl-8,11,13-podocarpatrien-13-ol) was obtained from Industrial Research (Lower Hutt, New Zealand), *trans*-parinaric acid (*t*-PnA), spin labels 5-doxyl-stearic acid (5-NS) and 16–doxyl-stearic acid (16-NS) from Molecular Probes (Eugene, OR), 5-methoxyindole from Sigma-Aldrich (St. Louis, MO) and the synthetic phospholipids 1,2-dimyristoyl-*sn*-glycero-3-[phospho-rac-glycerol] (DMPG) and 1,2-dimyristoyl-*sn*-glycero-3-phosphocholine (DMPC) from Avanti Polar Lipids (Birmingham, AL), and used as received. All other compounds were of analytical or spectroscopic reagent grade. Double-distilled and deionised water was used throughout this work.

2.2. Preparation and labelling of vesicles

Chloroform/methanol solutions containing 2.4 μmol of total phospholipid (DMPC or DMPG) and 0.1 μmol of (+)-totarol were dried under a stream of oxygen-free N_2 to obtain a thin film at the bottom of a small thick-walled glass tube, and the last traces of solvent were removed by keeping the samples under high vacuum for more than 3 h in the dark. Multilamellar vesicles (MLVs) were formed by resuspending the dried phospholipid in buffer (10 mM Hepes (pH 7.4), 100 mM NaCl, 0.1 mM EDTA) to a final concentration of 0.5 mM. The vesicle suspension was then heated at a temperature above the phase transition of the phospholipid and vortexed several times. Large unilamellar vesicles (LUVs) with a mean diameter of 90 nm were prepared from these MLVs by pressure extrusion through 0.1-μm polycarbonate filters (Nucleopore, Cambridge, MA). For energy transfer and partition experiments, (+)-totarol was externally added to pure phospholipid suspensions from aliquots of a (+)-totarol stock solution of 2.6×10^{-3} M in ethanol.

2.3. Spectroscopic measurements

Absorption spectra were carried out using a CAMSPEC M350 spectrophotometer. Fluorescence spectra, resonance energy transfer, quenching measurements and steady-state anisotropy, $\langle r \rangle$, were recorded with a SLM-8000C spectrofluorimeter fitted with Glan–Thompson polarisers. For the quantum yield determinations 5-methoxyindole was used as a reference ($\Phi_{ref} = 0.28 \pm 0.01$ [9]). Fluorescence decay measurements were carried out with a time-correlated single-photon timing system. Briefly, for exciting (+)-totarol at 285 nm, a frequency doubled, cavity dumped (3.7 MHz repetition rate), dye laser of rhodamine 6G (Coherent 701-2), synchronously pumped by a mode-locked Ar^+ laser (514.5 nm, Coherent Innova 400-10) was used. The emission at the magic angle was detected by a Hamamatsu R-2809 MCP photomultiplier at 320 nm (Jobin-Yvon HR320 monochromator). The instrumental response function (80 ps) was generated from a scatter dispersion (silica, colloidal water solution). The decay curves were collected into 1024 channels with 22.1 ps/channel and analysed using a non-linear least-squares iterative convolution method. The goodness of fit to a sum of exponentials was judged from the χ^2 and weighted residuals plots.

Mean lifetimes were determined according to Eq. 1:

$$\langle \tau \rangle = \frac{\sum \alpha_i \tau_i^2}{\sum \alpha_i \tau_i} \quad (1)$$

where α_i are the normalised pre-exponentials of each decay component τ_i.

The steady-state anisotropy $\langle r \rangle$, defined by Eq. 2 [10]

$$\langle r \rangle = \frac{(I_{VV} - G I_{VH})}{(I_{VV} + 2G I_{VH})} \quad (2)$$

was obtained by measuring the vertical and horizontal components of the fluorescence emission with excitation vertical and horizontal to the emission axis. The G factor ($G = I_{HV}/I_{HH}$) corrects for the transmissivity bias introduced by the detection system. These measurements were made with Glan–Thompson polarisers, and background intensities due to the lipid vesicles were always taken into account. Samples were excited at 270 nm and the polarised emission was detected at 320 nm.

2.4. Partitioning of (+)-totarol into vesicles

The increase in the fluorescence intensity observed for (+)-totarol in the presence of phospholipid vesicles as compared with that in the aqueous phase was used to quantify the phospholipid/water partition coefficient, K_P, according to Eq. 3:

$$\Delta I = \frac{\Delta I_{max}[L]}{1/(K_P \gamma) + [L]} \quad (3)$$

were ΔI ($\Delta I = I - I_0$) stands for the difference between the fluorescence intensity of the (+)-totarol molecule measured in the presence (I) and in the absence of the phospholipid vesicles (I_0). $\Delta I_{max} = I_\infty - I_0$ is the maximum value of this difference once the limiting value is reached (I_∞) upon increasing the phospholipid concentration [L], and γ is the molar volume of the phospholipid (for DMPG in the fluid phase the value of γ is 0.7 M^{-1} [11]).

2.5. Fluorescence quenching experiments

Quenching data were analysed by the Stern–Volmer plot of I_0/I versus $[Q]_L$, where I_0 and I stand for the fluorescence intensities in the absence and in the presence of the quencher, respectively, and $[Q]_L$ is the quencher (spin label) concentration in the phospholipid phase given by

$$[Q]_L = \frac{K_{PQ} V_T}{V_W + V_L K_{PQ}} [Q]_T \quad (4)$$

where $K_{PQ} = [Q_L]/[Q]_W$ is the partition coefficient of the quencher between the phospholipid phase and the aqueous phase, $[Q]_T$ is the concentration of the quencher in the total volume V_T ($V_T = V_L + V_W$) and V_L, V_W are, respectively, the volume of the lipid and aqueous phases. For 5-NS and 16-NS, K_{PQ} in the fluid phase is 89 000 and 9730, respectively [12] and for the purpose of obtaining V_L, a phospholipid molar volume of 0.9 M^{-1} for DMPC was used [13]. Experiments were carried out in DMPC/(+)-totarol LUVs at 30°C, by adding aliquots from a 8×10^{-4} M solution containing either the spin probes 16-NS or 5-NS in ethanol to the vesicle suspensions. Measure-

ments were carried out immediately after preparation.

2.6. Energy transfer measurements

The critical radius of transfer, R_0, was calculated from Eq. 5 [14]

$$R_0^6 = \frac{9000(\ln 10)\kappa^2 \Phi_D J}{128\pi^5 n^4 N_{AV}} \quad (5)$$

where Φ_D is the donor quantum yield in the absence of acceptor, n is the index of refraction of the medium, N_{AV} is Avogadro's number, κ^2 is the orientation factor and J corresponds to the degree of overlap between the donor emission spectrum and the acceptor absorption spectrum (overlap integral). This integral is given by Eq. 6:

$$J = \int_0^\infty f_D(\lambda)\varepsilon_A(\lambda)\lambda^4 d\lambda \quad (6)$$

where ε_A is the molar extinction coefficient of the acceptor and $f_D(\lambda)$ is the fluorescence spectrum of the donor normalised on the wavelength scale.

In order to obtain the theoretical expectation for energy transfer efficiency in a two dimensional system the approach of Snyder and Freire was used [15]. These authors adjusted practical polynomials to their results, and their fitting functions were used in this work. An exclusion parameter $\mathcal{L}$ (minimum distance allowed between donor and acceptor) was introduced in the derivation, but for $R_0/\mathcal{L} > 4$, its effect is negligible. In order to determine acceptor surface concentrations, an area of 0.7 nm^2 for the lipid headgroup of DMPC in the fluid phase was assumed [11]. For the determination of efficiencies of energy transfer, aliquots of *t*-PnA in ethanol were added to a cuvette containing the suspension of DMPC/(+)-totarol LUVs at 30°C, and the quenching of the (+)-totarol fluorescence emission was monitored upon excitation at 270 nm.

In a steady-state study of energy transfer eventual artefacts should be taken into account. In this way the effect of the acceptor (*t*-PnA) absorption at the donor ((+)-totarol) excitation wavelength (270 nm), was corrected according to Eq. 7 [16],

$$I_{corr}^D = I_{exp}^D \frac{A_T}{A_D} \frac{(1-10^{-A_D})}{(1-10^{-A_T})} \quad (7)$$

where I_{exp}^D is the experimentally obtained value, and A_D and A_T are the absorbances for the donor and total solution (donor and acceptor), respectively. The correction for the acceptor absorption of the donor emission (trivial process or reabsorption) was carried out as described in Eq. 8:

$$I_{corr}^D = I_{exp}^D \frac{2.303 A_A}{1-10^{-A_A}} \quad (8)$$

where A_A is now the absorption of the acceptor at the emission wavelength of the donor (310 nm).

3. Results

3.1. Photophysics of (+)-totarol in homogeneous solvents and in phospholipid model membranes

The absorption spectrum of (+)-totarol in ethanol shows a structureless absorption band in the 250–310 nm region, with a maximum at 281 nm ($\varepsilon = 2670$ M^{-1} cm^{-1}), characteristic of phenol derivatives. Fluorescence spectra in dilute solutions (4×10^{-5} M) were recorded in different aqueous solutions (pH 7.4), cyclohexane and ethanol (Fig. 2). Fluorescence in water and saline buffers was almost negligible (results not shown), becoming much more intense in cyclohexane and ethanol, being the fluorescence excitation and emission spectra in these two last solvents largely invariant. The fluorescent quantum yield of (+)-totarol was determined at

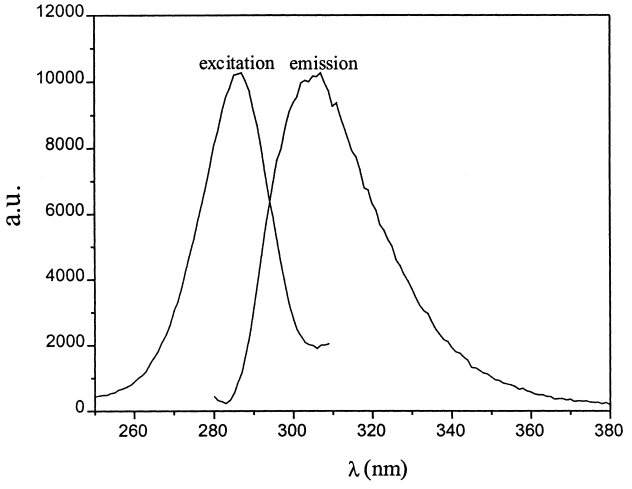

Fig. 2. Corrected fluorescence excitation ($\lambda_{em} = 315$ nm) and emission ($\lambda_{ex} = 275$ nm) spectra of (+)-totarol in ethanol.

Table 1
Photophysical parameters of (+)-totarol (quantum yield Φ, extinction coefficient ε, fluorescence lifetimes τ_i, and pre-exponential factors α_i,) in solution and incorporated into phospholipid vesicles of DMPC

Medium	Temp. (°C)	ε ($M^{-1}\,cm^{-1}$) (±100)	Φ (±0.01)	α_1 (±0.01)	τ_1 (ns) (±0.06)	α_2 (±0.01)	τ_2 (ns) (±0.2)	α_3 (±0.01)	τ_3 (ns) (±0.3)	$\langle\tau\rangle$ (±0.1)	χ^2
Ethanol	20	2670	0.26	0.05	0.61	0.95	3.5	–	–	3.5	1.2
Cyclohexane	20	n.d.	0.12	0.63	0.46	0.31	1.1	0.06	4.5	1.9	1.1
DMPC	20	n.d.	n.d.	0.02	0.64	0.98	3.7	–	–	3.7	1.3
DMPC	30	n.d.	n.d.	0.05	0.18	0.95	3.5	–	–	3.4	1.2

χ^2 is the goodness-of-fit parameter. See text for details. n.d., not determined.

room temperature in both solvents, cyclohexane and ethanol, being higher in the last protic solvent (Table 1). Similar behaviour has been reported for phenol [17] and other phenolic derivatives [18]. The quantum yield was temperature dependent (data not shown), decreasing as expected as the temperature was increased, in accordance with data reported for other phenolic molecules [19].

Fluorescence decay of (+)-totarol was recorded in cyclohexane and ethanol at 20°C, and the pre-exponential factors and lifetime values recovered from the fits are listed in Table 1. In cyclohexane it was necessary to use three components to describe the decay, at variance with ethanol where a clear bi-exponential kinetics was observed, consisting of a major kinetic component (95%) with a lifetime value of 3.5 ns, and a small contribution of a faster component. From the average lifetime $\langle\tau\rangle$ and the quantum yield a radiative fluorescence lifetime $\tau_0 = 14$ and a non-radiative rate constant $k_{nr} = 2\times10^7\ s^{-1}$ were estimated for (+)-totarol in ethanol at 20°C. An Arrhenius plot (not shown) of $\log(k_{nr})$ versus $1/T$ gave an activation energy to radiationless channels of 2.5 kcal/mol.

Absorption and fluorescence spectra of (+)-totarol in MLVs of DMPC and DMPG were recorded both below and above the lipid transition temperature. The shapes of the spectra were similar to those obtained in ethanol and cyclohexane and were not dependent on the phospholipid phase. No evidence of the ionised form (emission maximum at 345 nm) was observed. The fluorescence decay of (+)-totarol in the presence of vesicles of DMPC in gel and fluid phases was fitted to a two-exponential function (Table 1), although the major fraction of the decay relaxed through the longest lifetime component. The fluorescence lifetimes slowly decreased when temperature increased from 20°C to 30°C, i.e., when the phospholipid passed from the gel to the liquid-crystalline phase. It is interesting to note that the fluorescence data obtained for (+)-totarol in phospholipid vesicles were to a large extent similar to those obtained in a protic solvent like ethanol (Table 1).

3.2. Partition of (+)-totarol in phospholipid model membranes

Incorporation of (+)-totarol into the bilayer in the fluid phase was very fast, as observed from the increase in fluorescence intensity, taking place in 1–2 min both for DMPC and DMPG vesicles (results not shown). The increase in fluorescence intensity upon incorporation of (+)-totarol on both phospholipid model membranes was very similar, indicating that

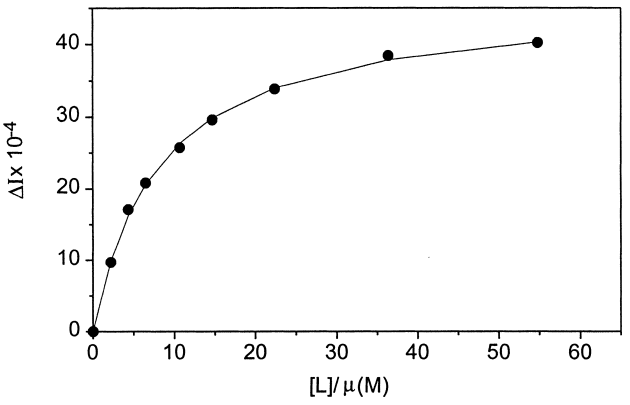

Fig. 3. Determination of the partition coefficient, K_P, of (+)-totarol from the fluorescence intensity increase upon incorporation to phospholipid LUVs of DMPG [L] at 30°C. ΔI stands for the difference between the fluorescence intensity of the (+)-totarol measured in the presence (I) and in the absence of lipid (I_0). The solid line is the best fit of Eq. 3 to the experimental data.

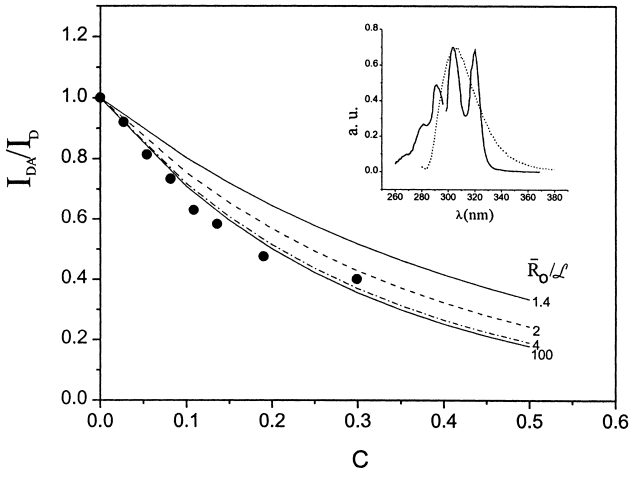

Fig. 4. Ratio of the (+)-totarol fluorescence intensity in the presence and absence of *t*-PnA (I_{DA}/I_D) as a function of *C*, the number of acceptors per $\bar{R}_0^2$ ($\bar{R}_0 = \Phi^{1/6}\ R_0$, see text for details). Experimental data are compared with the curves calculated for a random array of donors and acceptors for several values of $\bar{R}_0/\mathcal{L}$, where $\mathcal{L}$ is the distance of closest approach between donor and acceptor molecules. The spectral overlap between the fluorescence emission of (+)-totarol (···) and the absorption spectrum of *t*-PnA (———) in LUVs of DMPC is shown in the inset.

(+)-totarol incorporated with no dependence on the membrane charge in both anionic and zwitterionic phospholipids. The increase in the fluorescence intensity observed for (+)-totarol in the presence of phospholipid vesicles as compared with that in the aqueous phase was used to quantify the phospholipid/water partition coefficient, K_P (Eq. 3), from experiments where phospholipid concentration was varied while the (+)-totarol concentration was kept constant. Fig. 3 shows the enhancement in (+)-totarol fluorescence upon addition of phospholipid LUVs composed of DMPG at 30°C. From a two-parameter (ΔI_{max} and K_P) fitting procedure, a K_P value of $(1.8 \pm 0.2) \times 10^4$ was obtained. The same order of magnitude was found for DMPC (data not shown).

3.3. Fluorescence resonance energy transfer (FRET) from (+)-totarol to trans-parinaric acid

The fluorescent fatty acid *trans*-parinaric, *t*-PnA, was incorporated into LUVs of DMPC as a fluorescence resonance energy transfer (FRET) acceptor of (+)-totarol excitation. The overlap between the (+)-totarol fluorescence emission and the *t*-PnA absorption spectra is shown in Fig. 4 (inset), and a value of $J = 4.15 \times 10^{14}$ cm^3 M^{-1} was determined for the overlap integral (Eq. 6) considering a molar extinction coefficient of $\varepsilon = 76\,000$ M^{-1} cm^{-1} at 304 nm [20]. Assuming a quantum yield for (+)-totarol in the membrane of $\Phi = 0.26$ (the same value as in ethanol) and a local refractive index of $n = 1.425$ [21] the Förster radius, R_0, is 34 ± 1 Å (cf. Eq. 5), if an orientational factor $\kappa^2 = 2/3$ (dynamic isotropic limit) is considered. The FRET process between (+)-totarol and *t*-PnA was also confirmed by recording the excitation spectra of *t*-PnA in the DMPC/(+)-totarol samples and in DMPC bilayers. From the subtraction of both spectra, excitation spectrum of (+)-totarol was obtained (data not shown).

The FRET data were used to investigate the distribution of *t*-PnA (acceptor) around the (+)-totarol (donor) molecule, namely the possibility of a non-random distribution of acceptor in the phospholipid membrane. Following Snyder and Freire [15], the ratio of the (+)-totarol fluorescence intensity in the presence and absence of acceptors (I_{DA}/I_D) was plotted as a function of *C*, i.e., the number of acceptors per $\bar{R}_0^2$, where $\bar{R}_0 = \Phi^{1/6}\ R_0$ (Fig. 4). The experimental data were compared with the curves calculated for a random array of donors and acceptors for several values of $\bar{R}_0^2/\mathcal{L}$, where $\mathcal{L}$ is the distance of closest approach between donor and acceptor molecules. As shown in Fig. 4, the theoretical expectation when no significant exclusion distance is considered, largely agrees with the experimental results.

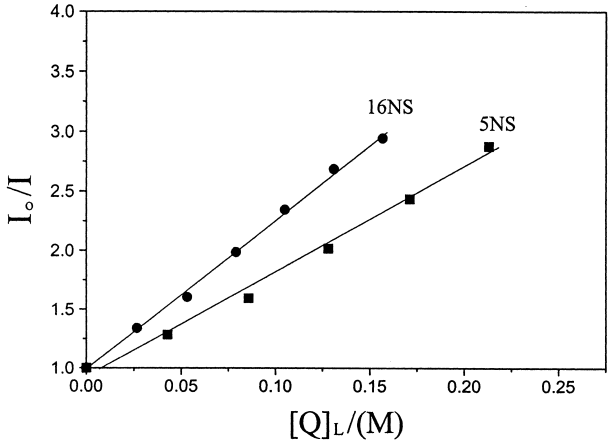

Fig. 5. Stern–Volmer plot for the quenching of (+)-totarol by 5-NS and 16-NS in lipid vesicles of DMPC at 30°C.

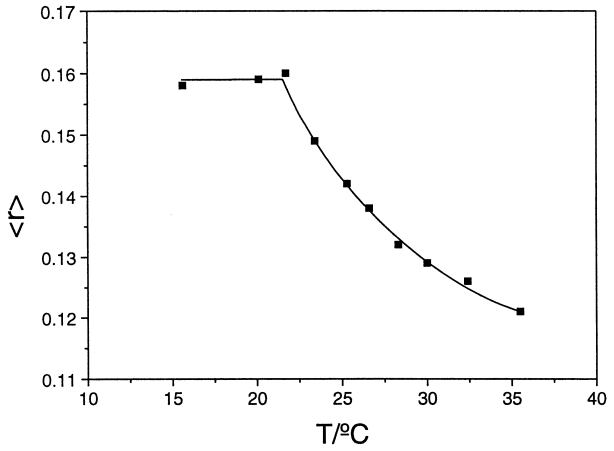

Fig. 6. Dependence of the fluorescence steady-state anisotropy $\langle r \rangle$ of (+)-totarol in DMPC model membranes with temperature.

3.4. Differential quenching experiments

The transverse location (penetration) of (+)-totarol into the lipid bilayer was investigated by monitoring the relative quenching of the fluorescence of (+)-totarol incorporated in the fluid phase of DMPC by the lipophilic spin probes 5-NS and 16-NS. The addition of any of the two nitroxide quenchers resulted in a decrease of the (+)-totarol fluorescence. The Stern–Volmer plots of the fluorescence intensity changes were linear (see Fig. 5) and the Stern–Volmer constants (K_{SV}) were obtained from their slopes. The ratio of these constants, $K_{SV(16-NS)}/K_{SV(5-NS)}$, was found to be 1.4. It can be seen that 5-NS, which has its nitroxide group at carbon-5, quenches (+)-totarol fluorescence less efficiently than 16-NS, pointing out that (+)-totarol is located in the phospholipid membrane far away from the phospholipid/water interface.

3.5. Steady-state anisotropy measurements

The steady-state fluorescence anisotropy, $\langle r \rangle$, of (+)-totarol in MLVs of DMPC was recorded as a function of temperature (Fig. 6). Anisotropy was approximately constant from 15°C to 22°C, showing a significant decrease at 23°C. The sharp change observed indicates that (+)-totarol adequately reports the phase transition of the membrane, increasing its rotational mobility on going from the gel to the fluid phase and confirms the location of the molecule incorporated into the phospholipid palisade of the membrane. These results also suggest that, at the concentration used (4 mol%), (+)-totarol is randomly distributed around the phospholipids showing no specific preference for either of the two lipid phases.

4. Discussion

In this work we have studied the location and interaction of (+)-totarol, a bioactive diterpenoid molecule, when incorporated into phospholipid model membranes by means of its intrinsic fluorescence. We first determined some of its fluorescence properties in homogeneous solvents in order to obtain enough data that could be used to conclude about its microenvironment in the phospholipid systems. As expected from the (+)-totarol structure, the majority of its photophysical parameters were similar to those of phenol or other phenol related relevant biological compounds such as tyrosine [19] or α-tocopherol [18]. Upon increasing the solvent polarity (with the exception of water) or decreasing temperature, both the quantum yield and lifetime (Table 1) of (+)-totarol increased, the same being reported previously for phenol [17,22]. The behaviour of the fluorescence decay of (+)-totarol in homogeneous solvents is more complex than that observed for other phenol derivatives. Phenol, *p*-cresol and anisol exhibit monoexponential decay kinetics while for COOH-substituted compounds two exponentials are required [23,24]. The origin of the complex fluorescence kinetics of (+)-totarol in cyclohexane is not clear. It could be explained assuming the formation of (+)-totarol aggregates in the solvent, but, as it is discussed below, the fluorescence spectra recorded in cyclohexane do not support this hypothesis. In ethanol and phospholipid bilayers the fluorescence decay is bi-exponential but is dominated by a longer lifetime component of 3.5 ns, similar to that obtained for phenol and *p*-cresol, which comprises 99% or more of the total decay of (+)-totarol. The origin of the short lifetime component is not due apparently to impurities in the sample, since the compound was chromatographically pure. It cannot be also attributed to intramolecular quenching, as it has been postulated for tyrosine analogues [24] since (+)-totarol does not contain carboxyl groups. Similar bi-ex-

ponential behaviour has been also reported for other fluorescent molecules, such as diphenylhexatriene and *t*-PnA, and its origin remains yet unknown [25,26].

As concluded from the partition coefficient study, (+)-totarol incorporates very efficiently into phospholipidic systems, and the high value obtained, $K_P = 1.8 \pm 0.2 \times 10^4$, is compatible with its very hydrophobic structure (Fig. 1), the hydroxyl group being the only polar group of the molecule. No variation of behaviour was found with both anionic and zwitterionic phospholipids, ruling out the involvement of electrostatic interactions between this neutral compound and neither of both types of phospholipid. At the phospholipid concentration used in this work, the partition equilibrium is largely shifted from the water to the membrane, and from the differential quenching study, a non-shallow location for (+)-totarol is concluded. The nitroxide quenchers 16-NS and 5-NS are known to be located at the interior and near the surface respectively of the bilayer [27]. We have found that 16-NS quenches (+)-totarol fluorescence much more effectively than 5-NS as should be expected if the phenolic moiety of the molecule is located in a transversal location far away from the lipid-water interface. This fact is in agreement with the significant anisotropy variation found on (+)-totarol when the phospholipid passes through the gel to liquid–crystalline phase transition. For a similar fluorophore such as α-tocopherol, it has been reported that, upon increasing its concentration in a non-polar solvent such as cyclohexane, evidence for aggregate formation is obtained from the absorption spectrum, since a shift from a monomeric band at 283 nm to a new band at 295 nm is observed [18]. At the concentration range where we have carried out the present study, no evidence for such an aggregate was obtained, even considering that the hydrophobic terpenoid structure is internalised in the membrane. Both fluorescence lifetime and spectra of (+)-totarol when incorporated into the membrane are similar to those found in ethanol, suggesting that the molecule could be involved in hydrogen bond interaction. This hydrogen bond interaction could be originated by inter-(+)-totarol interactions, although hydrogen bond interaction with the carbonyl moieties of the phospholipid should not be ruled out.

We have also studied the possible formation of complexes with a model system including the unsaturated fatty acid, *t*-PnA, since (+)-totarol is a protector against oxidative stress. The formation of complexes with unsaturated fatty acids has been reported for other oxidative protector molecules such as α-tocopherol [28,29]. Resonance energy transfer is a useful methodology, since *t*-PnA (a tetraene) is an efficient acceptor of (+)-totarol, being its critical radius of transfer $R_0 = 34 \pm 1$ Å. In addition, other approaches such as the observation of spectral alterations in the absorption or emission cannot be used, once the molecular interaction is not expected to induce orbital mixing. The model we used assumes that the system is strictly planar, i.e., both donor and acceptor are incorporated at the same depth in the membrane. More refined models taking explicitly into account the internalisation of the donor could be fitted to the data [13], but for the purpose of the evaluation of aggregate formation ((+)-totarol plus unsaturated molecule), this detail is not needed. In addition, the acceptor is also deeply internalised in the membrane [30], and the donor-acceptor interplanar distance should be negligible. The efficiency of energy transfer is correctly predicted on the basis of a random distribution of acceptors around the (+)-totarol donor (Fig. 4). In this way, a strong interaction such as the formation of dimers or other aggregates is ruled out, once it would increase the efficiency of transfer leading to a significant deviation between data and theoretical expectation, i.e., a greater fluorescence quenching. On the other hand, the existence of an excluding distance $\mathcal{L}$, was not expected, and it is not observed. This parameter could only report the formation of enriched domains of *t*-PnA away from the donor which is a very unlikely process.

In summary, the fluorescence properties of (+)-totarol are very similar to those reported for other phenol-derivatives and the (+)-totarol molecule shows a high preference for phospholipid systems that is not mediated through electrostatic interactions. The sharp change observed in the steady-state-anisotropy during the lipid phase transition, together with the results obtained from the quenching experiments suggest that (+)-totarol is deeply embedded in the membrane, with the phenol group located distant to the phospholipid/water interface.

Once this phenolic moiety is essential for the antibacterial activity, we can conclude that the action of (+)-totarol is mediated through its interaction with membranes by perturbing the membrane structure, weakening the Van der Waals interactions between the phospholipid chains. Recent results obtained in our laboratory [8] support this assumption.

Acknowledgements

This investigation was supported by Grant PM98-0100 from DGESIC, Madrid (to J.V.) and by funding from the Colgate Company, Piscataway, NJ (Zürich). We thank Drs Aleksander Fedorov and Luis M.S. Loura (Centro de Química-Física Molecular, Lisboa) for their kind help with the time-resolved fluorescence measurements and data analysis, and Professor Dr B. Guggenheim, Director of the Institut für orale Mikrobiologie und allgemeine Immunologie, for encouragement.

References

[1] S. Shapiro, B. Guggenheim, Quant. Struct.-Act. Relat. 17 (1998) 327–337.
[2] I. Kubo, H. Muroi, M. Himejima, J. Nat. Prod. 55 (1992) 1436–1440.
[3] G.B. Evans, H. Furneaux, M.B. Gravestock, G.P. Lynch, G.K. Scott, Bioorg. Med. Chem. 7 (1999) 1953–1964.
[4] H. Muroi, I. Kubo, J. Appl. Bacteriol. 80 (1996) 387–394.
[5] K. Nicolson, G. Evans, P.W. O'Toole, FEMS Microbiol. Lett. 15 (1999) 233–239.
[6] H. Haraguchi, H. Ishikawa, S. Sakai, B.P. Ying, I. Kubo, Experientia 15 (1996) 573–576.
[7] H. Haraguchi, H. Ishikawa, I. Kubo, Plant. Med. 63 (1997) 213–215.
[8] V. Micol, C.R. Mateo, S. Shapiro, F.J. Aranda, J. Villalaín, Biochim. Biophys. Acta (2000) submitted.
[9] J.N. Demas, G.A. Crosby, J. Phys. Chem. 75 (1971) 991–1024.
[10] J.R. Lackowicz, Principles of Fluorescence Spectroscopy, Plenum, New York, 1983, pp. 262–268.
[11] D. Marsh, Handbook of Lipid Bilayers, CRC Press, Boca Raton, FL, 1990.
[12] J.R. Wardlaw, W.H. Sawyer, K.P. Ghiggino, FEBS Lett. 231 (1987) 20–24.
[13] L. Davenport, R.E. Dale, R.H. Bisby, R.B. Cundall, Biochemistry 24 (1985) 4097–4108.
[14] T. Förster, Discuss. Faraday Soc. 27 (1959) 7–17.
[15] B. Snyder, E. Freire, Biophys. J. 40 (1982) 137–148.
[16] A. Coutinho, M. Prieto, J. Chem. Ed. 70 (1993) 425–428.
[17] C.A. Parker, Photoluminescence of Solutions, Elsevier, Amsterdam, 1968, pp. 262–268.
[18] F.J. Aranda, A. Coutinho, M.N. Berberan-Santos, M. Prieto, J.C. Gómez-Fernández, Biochim. Biophys. Acta 985 (1989) 26–32.
[19] D. Creed, Photochem. Photobiol. 39 (1984) 563–575.
[20] L.A. Sklar, B.S. Hudson, M. Petersen, J. Diamond, Biochemistry 16 (1977) 813–818.
[21] D. Toptygin, L. Brand, J. Fluoresc. 5 (1995) 39–50.
[22] J.B. Berlman, Handbook of Fluorescence Spectra of Aromatic Molecules, Academic Press, New York, 1965, pp. 61–62.
[23] P. Gauduchon, Ph. Wahl, Biophys. Chem. 8 (1978) 87–104.
[24] W.R. Laws, J.B.A. Ross, H.R. Wyssbrod, J.M. Beechem, L. Brand, Biochemistry 25 (1986) 599–607.
[25] T. Parasassi, G. De Stasio, R.M. Rusch, E. Gratton, Biophys. J. 59 (1991) 466–475.
[26] C.R. Mateo, J.C. Brochon, M.P. Lillo, A.U. Acuña, Biophys. J. 65 (1993) 2237–2247.
[27] J.F. Ellena, S.J. Archer, R.N. Dominey, B.D. Hill, D.S. Cafiso, Biochim. Biophys. Acta 940 (1988) 63–70.
[28] S. Urano, M. Iida, I. Otani, M. Matsuo, Biochem. Biophys. Res. Commun. 146 (1987) 1413–1418.
[29] W. Stillwell, W. Ehringer, S.R. Wassall, Biochim. Biophys. Acta 1105 (1992) 237–244.
[30] M. Castanho, M. Prieto, A.U. Acuña, Biochim. Biophys. Acta 1279 (1996) 164–168.